ChemPubSoc Europe

DOI: 10.1002/chem.201804121

CHEMISTRY A European Journal Full Paper

Alloys

Pressure-Induced Stable Binary Compounds of Magnesium and Germanium

Chao Wang,*[a] Yunxian Liu,[a] Pin Lv,[a] Hairui Sun,[a] and Defang Duan*[b]

Abstract: Motivated by the possibility to obtain unusual stoichiometric compounds (e.g., Na–Cl and Mg–O systems) with exotic properties at high pressures, we systematically investigated the high-pressure structures and chemical bonding of Mg–Ge systems by using a structure-searching method and first-principles calculations. Compared with the stable composition of Mg_2Ge at ambient pressure, several stoichiometries (e.g., Mg_3Ge, MgGe, and $MgGe_2$) were predicted to be stable under high pressures. The $Pm\bar{3}m$ Mg_3Ge structure consists of a 12-fold-coordinated face-sharing $GeMg_{12}$ cuboctahedron, whereas the *P*4/*mmm* MgGe and *Cmcm* $MgGe_2$ phases form $MgGe_8$ hexahedrons and $MgGe_4$ polygons, respectively. All the stable phases of Mg–Ge compounds under high pressures exhibit metallic features owing to overlap between the conduction and valence bands. For *Cmcm* $MgGe_2$, the projected density of states near the Fermi energy mainly derive from Ge s, Ge p, and Ge d, which are responsible for its metallicity. The calculated superconducting critical temperature values of *Cmcm* Mg_2Ge and *P*4/*mmm* MgGe reach 10.3 and 9.07 K at 5 GPa, respectively.

Introduction

Magnesium compounds have been intensively studied in the fields of physics, chemistry, and materials science owing to their potential applications. For instance, Mg–Li alloys can be used in the automotive, aerospace, and electronic industries.[1] Magnesium peroxide (MgO_2) is widely applied in the agricultural and environmental industries owing to the fact that it can stably release oxygen.[2] Mg_2X (X = Si, Ge, and Sn) are considered to be candidates for high-performance thermoelectric materials because of their large Seebeck coefficients, low electrical resistivity, and low thermal conductivity.[3–5] Moreover, as narrow-band-gap semiconductors, Mg_2X (X = Si, Ge, and Sn) can be utilized as infrared detectors for optical fibers.[6] Mg–Al alloys are widely used in many kinds of industries as a result of their good formability, weldability, mechanical strength, and corrosion resistance.[7] Therefore, the search for new magnesium compounds with exotic properties has been the focus of much research.

Pressure is an important thermodynamic parameter that has become a powerful tool to obtain unconventional stoichiometric compounds with unexpected properties or structural features by shortening the interatomic distances in the materials. Recently, some magnesium compounds were investigated in theory and experiment at high pressures; for example, a new monoclinic *C*2/*m* structure of Mg_2C_3 was synthesized under high-pressure and high-temperature conditions, and it contains linear C_3^{4-} chains.[8] Theoretical work performed by Tse et al. indicated that metallic Mg_2C and MgC_2 transformed into semiconductors, whereas Mg_2C_3 underwent an insulator–metal transition under pressure.[9] Moreover, a binary Mg–N compound, in which the Mg atoms played an important role in the stabilization of polymeric nitrogen networks, was explored up to 300 GPa. Two stoichiometries (i.e., MgN_3 and MgN_4) were proposed to be potential high-energy-density materials with energy densities of 2.87 and 2.08 kJ g^{-1}, respectively.[10] Zhu et al. reported that, except for MgO, two extraordinary compounds of the Mg–O system, namely, MgO_2 and Mg_3O_2, were theoretically predicted to be stable at 116 and 500 GPa, respectively.[11] Magnesium polyhydrides have been extensively studied, and the critical temperature (T_c) values of MgH_2, MgH_4, and MgH_{12} were reported to be 16–23, approximately 10, and 47–60 K at different pressures.[12,13] Furthermore, in addition to Mg_2Si, several compounds such as $MgSi_2$, MgSi, and Mg_9Si become stable at finite pressures, and $MgSi_2$ is a potential superconductor with a T_c up to approximately 7 K.[14] The investigations of the above magnesium compounds prompted us to search for new magnesium compounds with intriguing properties under high pressures. To our best knowledge, although the high-pressure phase transitions of Mg_2Ge have been studied,[15,16] the relative stabilities, novel structures, and properties of magnesium–germanium (Mg–Ge) compounds with wide compositions under high pressures have not yet been well explored.

[a] Dr. C. Wang, Dr. Y. Liu, Dr. P. Lv, Dr. H. Sun
School of Physics and Physical Engineering, Qufu Normal University
Qufu, 273165 (P.R. China)
E-mail: wangchao2016@qfnu.edu.cn

[b] Prof. D. Duan
State Key Laboratory of Superhard Materials, College of Physics
Jilin University, Changchun, 130012 (P.R. China)
E-mail: duandf@jlu.edu.cn

Supporting Information and the ORCID identification number(s) for the author(s) of this article can be found under: https://doi.org/10.1002/chem.201804121.

In this work, the high-pressure phase diagram of the Mg–Ge system was explored by the evolutionary algorithm Universal Structure Predictor: Evolutionary Xtallography (USPEX).[17–19] Several stoichiometries (e.g., Mg_2Ge, Mg_3Ge, MgGe, and $MgGe_2$) were predicted. The *Pm*$\bar{3}$*m* Mg_3Ge, *P*6$_3$/*mmc* Mg_2Ge, *P*4/*mmm* MgGe, and *Cmcm* $MgGe_2$ structures constitute a $GeMg_{12}$ cuboctahedron, $MgGe_3$ polygons, $MgGe_8$ hexahedrons, and $MgGe_4$ polygons, respectively. The bonding nature of the Mg–Ge compounds was investigated with charges transferring from the Mg atom to the Ge atom. Electron–phonon calculations showed that the T_c values of *Cmcm* Mg_2Ge and *P*4/*mmm* MgGe were 10.3 and 9.07 K at 5 GPa, respectively.

Results and Discussion

Phase stability of Mg–Ge compounds at high pressures

The stable stoichiometries and structures for Mg_xGe_y ($x = 1$–4, $y = 1$–2) were investigated up to 200 GPa at 0 K. Then, the formation enthalpy (ΔH_f) relative to elemental Mg and Ge solids for all predicted structures in each chosen stoichiometry were evaluated according to Equation (1):

$$\Delta H_f(Mg_xGe_y) = [H(Mg_xGe_y) - x\,H(Mg) - y\,H(Ge)]/(x+y) \qquad (1)$$

The enthalpies of *P*6$_3$/*mmc* and *Im*$\bar{3}$*m* for Mg and *Fd*$\bar{3}$*m* and *Cmca* for Ge were selected as the thermodynamic references. Normally, the convex hull is constructed by the calculated enthalpies of the most stable structures for each stoichiometry. At a given pressure, structures for which the formation enthalpies are located on the convex hull (solid lines) are considered to be thermodynamically stable and can be synthesized experimentally, whereas the phases above the convex hull (dotted line) are supposed to be metastable. The formation enthalpies (ΔH) of various Mg–Ge compounds are presented in Figure 1 and Figure S1 (Supporting Information). Moreover, magnification of the convex hull at 5, 50, 100, and 200 GPa and the stable pressure ranges of the corresponding structures are shown in Figure S2 (Supporting Information). Our main results can be summarized as follows: 1) except for the fact that the known Mg_2Ge stoichiometry is energetically stable at 0 GPa, Mg_3Ge is stable and emerges on the convex hull (Figure S1); 2) at 5 GPa, the Mg_3Ge, Mg_2Ge, and MgGe stoichiometries are thermodynamically stable species, whereas Mg_4Ge and $MgGe_2$ lie above the hull, which is indicative of their instability (Figure 1); 3) up to 50 GPa, in addition to the stable compounds (i.e., Mg_3Ge, Mg_2Ge, and MgGe), $MgGe_2$ is located on the convex hull; 4) At 100, 150, and 200 GPa, the stable compositions are the same as those at 50 GPa. Furthermore, we predicted the known structures (*Fm*$\bar{3}$*m*, *Pnma*, and *P*6$_3$/*mmc*) of Mg_2Ge and gave the enthalpy curves of the structures relative to *Pnma* as a function of pressure, as graphed in Figure S3. It can be seen that Mg_2Ge transforms from *Fm*$\bar{3}$*m* into *Pnma* at approximately 6 GPa and then into *P*6$_3$/*mmc* at 39 GPa, which is in accordance with previous work (Mg_2Ge goes through two phase transitions under pressure).[16]

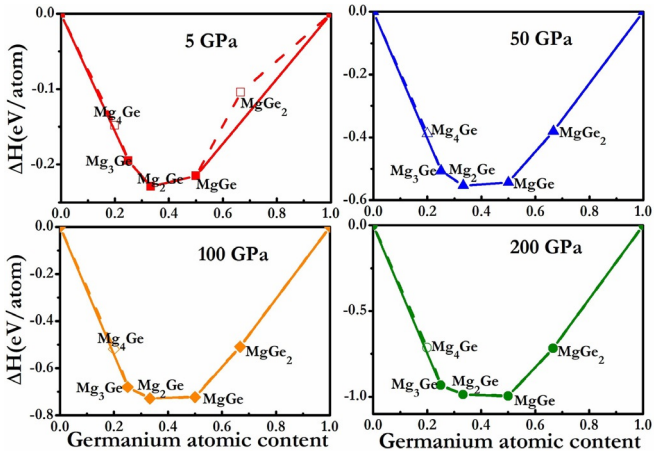

Figure 1. Formation enthalpies (ΔH) of various Mg–Ge compounds with respect to decomposition into the constituent elemental solids.

Structures and dynamical stabilities of Mg–Ge compounds

For Mg_3Ge, we predicted an energetically favored *Pm*$\bar{3}$*m* structure (Figure 2a) that is stable above 18 GPa (Figure S2b). There are 12 Mg atoms surrounding each Ge atom to form a face-sharing Ge–Mg cuboctahedron, wherein the Mg–Ge distance is 2.494 Å. Figure 2b gives the high-pressure phase of Mg_2Ge; it adopts a Ni_2In-type (*P*6$_3$/*mmc*) structure, in which two inequivalent Mg atoms occupy the 2d and 2a sites and the Ge atoms are located at the 2c sites to form $MgGe_3$ polygons. The nearest Mg–Ge distance is 2.274 Å. Turning to the MgGe stoichiometry, a tetragonal *P*4/*mmm* phase was predicted to be stable in the pressure range of 4 to 200 GPa (Figure S2b), wherein the Mg atoms are situated at the position of the vertex, whereas the Ge atoms are located in the body center (Figure 2c). Moreover, each Mg atom is eightfold coordinated by Ge, constituting $MgGe_8$ hexahedrons with a Mg–Ge distance of 2.489 Å.

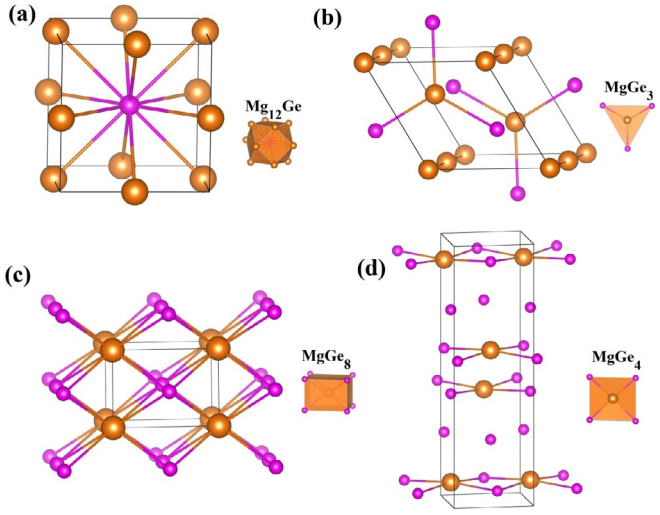

Figure 2. Crystal structures of Mg–Ge compounds in their stable regions. a) *Pm*$\bar{3}$*m* structure of Mg_3Ge. b) *P*6$_3$/*mmc* structure of Mg_2Ge. c) *P*4/*mmm* structure of MgGe. d) *Cmcm* structure of $MgGe_2$. In all the structures, the large orange and small pink balls represent Mg and Ge atoms, respectively.

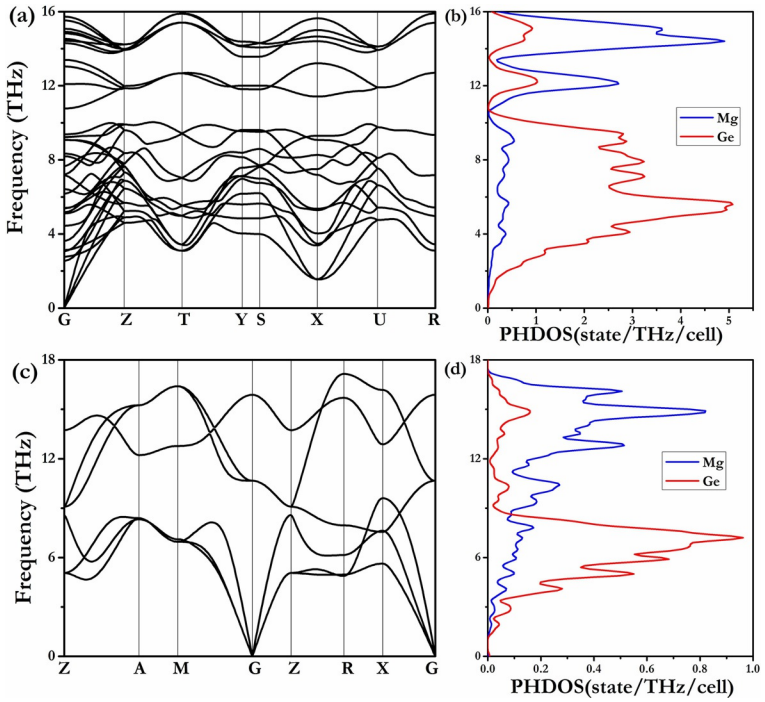

Figure 3. Phonon dispersion curves and partial phonon density of states (PHDOS) of a, b) *Cmcm* $MgGe_2$ and c, d) *P4/mmm* MgGe at different pressures.

The preferred stable structure of $MgGe_2$ is an orthogonal structure (space group *Cmcm*) that forms a $MgGe_4$ layer and a Ge layer, as shown in Figure 2d. The lattice parameters and atomic positions of Mg–Ge compounds are listed in Table S1.

To judge the dynamic stabilities of the Mg–Ge compounds, we calculated their phonon spectra with the supercell method by using the quasiharmonic mode. No imaginary phonon frequency was observed in the whole Brillouin zone, as seen in Figure 3 and Figure S4, which suggests that they are all dynamically stable in their accessible pressures. Besides, it can be seen that the low phonon mode is mainly from Ge, whereas the motion of Mg is the major contributor to the high-frequency regimes; this is a result of the fact that germanium is much heavier than magnesium.

Electronic properties and chemical bonds of Mg–Ge compounds

To provide insight into the electronic properties of the Mg–Ge compounds, the electronic band structures and the corresponding projected density of states (PDOS) were calculated, as presented in Figure 4 and Figures S5 and S6. We found that the stable $Pm\bar{3}m$ Mg_3Ge, $P6_3/mmc$ Mg_2Ge, *P4/mmm* MgGe, and *Cmcm* $MgGe_2$ phases were metallic with overlap between the conduction and valence bands. As for *Cmcm* $MgGe_2$, the PDOS near the Fermi energy mainly derives from Ge s, Ge p, and Ge d, which are responsible for its metallicity, whereas the Mg s, Mg p, and Mg d states make small contributions, as shown in Figure 4a. To prove this, a hypothetical model of Mg_0Ge_2 was constructed, wherein all Mg atoms were removed from the *Cmcm* $MgGe_2$ phase. The calculated PDOS revealed that *Cmcm* Mg_0Ge_2 still possesses metallicity (Figure 4b). *P4/mmm* MgGe was found to exhibit similar electronic properties (Figure 4e).

To obtain deeper insight into the chemical bonds in *Cmcm* $MgGe_2$ and *P4/mmm* MgGe, the electron location function (ELF) was calculated. Generally, ELF values above 0.5 between the nearest atoms are indicative of lone pairs of electrons, core electrons, or covalent bonds, whereas small ELF values (<0.5) correspond to ionic bonds. As illustrated in Figure 4c, f, the ELF values between Mg and Ge are small (<0.5), which is typical of ionic bonds. Then, we also calculated the difference charge density (crystal density minus superposition of isolated atomic densities) of *Cmcm* $MgGe_2$, as shown in Figure 4d. It can be seen that charge is transferred from Mg to the Ge atoms, which is further supported by the results of the Bader charge calculation (Table S2). In addition, the calculated ELF of $Pm\bar{3}m$ Mg_3Ge and $P6_3/mmc$ Mg_2Ge can be seen in Figure S7.

Superconductivity of Mg–Ge compounds

To explore the possible superconductivity of the Mg–Ge compounds, the electron–phonon coupling (EPC) parameter (λ), the logarithmic average phonon frequency (ω_{log}), and the electronic density of states at the fermi level [$N(E_f)$] were calculated. We estimated the T_c values by using the Allen–Dynes-modified McMillan equation. For the rich Mg compounds (i.e., Mg_3Ge and Mg_2Ge), superconductivities were not found, whereas for $MgGe_2$ and MgGe, by using the nominal Coulomb pseudopotential parameter (μ^*) of 0.1 along with the calculated ω_{log} (217.12 and 257.75 K) and λ (0.51 and 0.4) values, the resultant T_c values of *Cmcm* Mg_2Ge and *P4/mmm* MgGe at 5 GPa were predicted to be 10.3 and 9.07 K, respectively. To investigate the effect of pressure on superconductivity, the tendency of T_c with pressure for *Cmcm* Mg_2Ge and *P4/mmm* MgGe was explored. The values of λ, ω_{log}, $N(E_f)$, and T_c at various pressures are listed in Table 1. The results show that the values of T_c for the *Cmcm* Mg_2Ge and *P4/mmm* MgGe structures decrease with increasing pressure. It can be seen that upon compression, the values of the average frequency (ω_{log}) increase, but the calculated λ and $N(E_f)$ values decrease. Therefore, we think that the T_c values decrease with pressure as a result of a decreases in both λ and $N(E_f)$.

Conclusion

In conclusion, we systematically investigated Mg_xGe_y ($x=1$–4, $y=1$–2) systems up to 200 GPa. Aside for the known Mg_2Ge composition, the three Mg_3Ge, MgGe, and $MgGe_2$ stoichiometries were predicted to be stable under high pressures. Moreover, the $Pm\bar{3}m$ Mg_3Ge, *P4/mmm* MgGe, and *Cmcm* $MgGe_2$ structures form a 12-fold-coordinated face-sharing $GeMg_{12}$ cu-

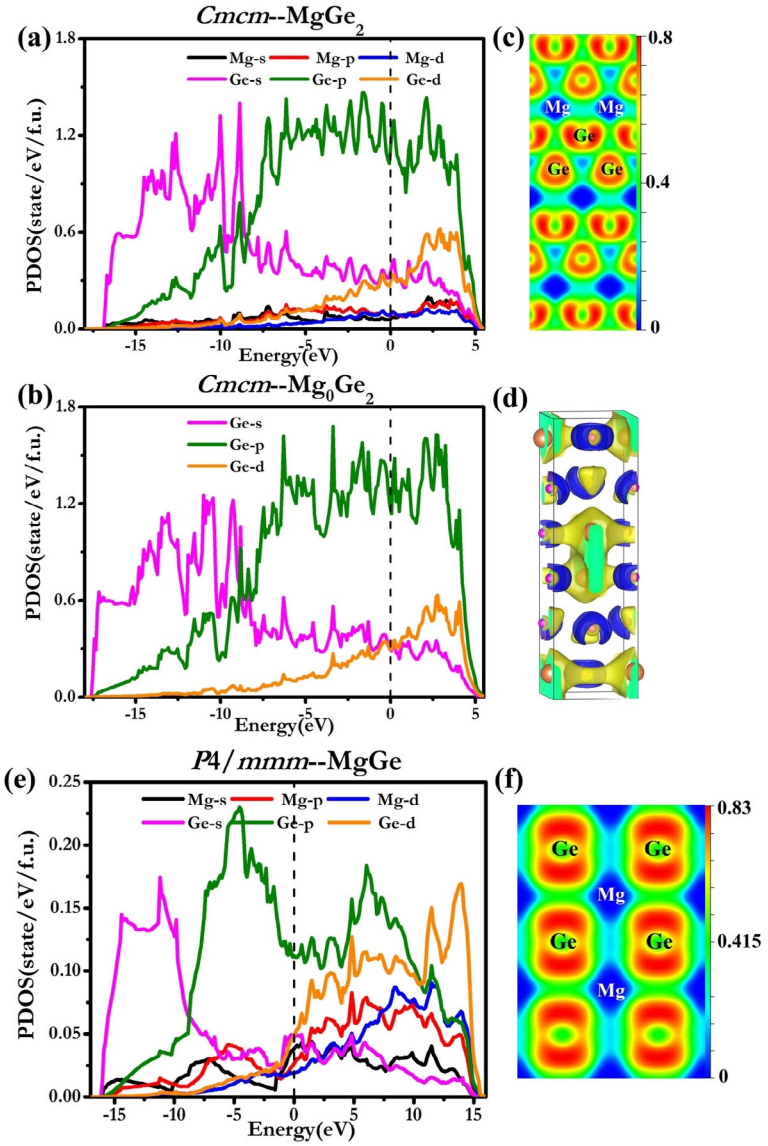

Figure 4. Electronic structures and chemical bonding of Mg–Ge compounds. a, b) The calculated projected density of states (PDOS) of *Cmcm* $MgGe_2$ and *Cmcm* Mg_0Ge_2. c, d) The electron localization function (ELF) and difference charge density maps of *Cmcm* $MgGe_2$. e, f) The calculated PDOS and ELF of *P4/mmm* MgGe.

Table 1. The calculated electron–phonon coupling parameter (λ), logarithmic average phonon frequency (ω_{log}), electronic density of states at the fermi level [$N(E_f)$, states/spin/Ry/unit cell], and superconducting critical temperature (T_c) values of *Cmcm* $MgGe_2$ and *P4/mmm* MgGe at different pressures.

Structure	P [GPa]	λ	ω_{log} [K]	$N(E_f)$	T_c [K] ($\mu^*=0.1$)
Cmcm $MgGe_2$	5	1.46	92.70	15.74	10.3
	50	0.51	217.12	12.02	2.82
	100	0.35	287.56	10.37	0.53
	150	0.29	338.79	9.66	0.11
	200	0.25	378.75	9.05	0.02
P4/mmm MgGe	5	1.04	122.91	4.87	9.07
	50	0.40	257.75	3.80	1.04
	100	0.27	332.20	3.32	0.06
	150	0.23	385.65	3.31	0.007
	200	0.20	432.16	3.00	0

boctahedron, $MgGe_8$ hexahedrons, and $MgGe_4$ polygons, respectively. The *Cmcm* Mg_2Ge and *P4/mmm* MgGe structures are superconductors with T_c values of 10.3 and 9.07 K at 5 GPa, respectively. This work provides insight into the structural features and properties of Mg–Ge systems under pressure.

Computational Details

In this paper, all calculations were performed within the framework of density functional theory (DFT). To search all potential stable ground-state structures of the Mg–Ge system, an ab initio variable-composition evolutionary method USPEX was performed at 50, 100, 150, and 200 GPa.[17–19] Its success was demonstrated by determining the stable structures of the various compounds.[20–24] All structural optimizations, calculations of the enthalpies, electronic calculations, and other structural property calculations were performed with the Vienna ab initio simulation package (VASP).[25] The Perdew–Burke–Ernzerhof generalized gradient approximation (GGA)[26] was chosen as the exchange-correlation functional, and projector-augmented wave (PAW)[27] potentials were adopted to describe the ionic potentials. The electron configurations of $3s^2$ and $4s^24p^2$ for Mg and Ge, respectively, were chosen as valence states. A kinetic energy cutoff of 500 eV for the plane-wave basis-set expansion and Monkhorst–Pack k meshes spacing of $2\pi\times0.03$ Å^{-1} were adopted, which made sure that all enthalpy calculations were well converged. The dynamical stabilities of the Mg–Ge compounds were investigated through phonon calculations based on the supercell approach[28] by using the PHONOPY code.[29] The degree of electron localization was gauged by means of the electron localization function (ELF).[30] Bader charge analysis[31–33] was applied to calculate the electronic charge transfer. The electron–phonon coupling (EPC) calculations were employed with the density function perturbation theory by the Quantum ESPRESSO code.[34] The norm-conserving pseudopotentials with a kinetic energy cutoff of 90 Ry were used. The q-point mesh in the first Brillouin zone of $3\times3\times3$ and $4\times4\times3$ for *Cmcm* $MgGe_2$ and *P4/mmm* MgGe, respectively, were adopted. The transition temperature (T_c) values were estimated by using the Allen–Dynes-modified McMillan equation [Eq. (2)],[35] which is accurate for materials with $\lambda < 1.5$.

$$T_C = \frac{\omega_{log}}{1.2}\exp\left[-\frac{1.04(1+\lambda)}{\lambda-\mu^*(1+0.62\lambda)}\right] \quad (2)$$

Acknowledgements

This work was supported by the National Natural Science Foundation of China (Nos. 11704220, 11804185, and 11674122), and by the Natural Science Foundation of Shandong Province of China (Grant Nos. ZR2017BA020, ZR2018PA010, and ZR2017BA012).

Conflict of interest

The authors declare no conflict of interest.

Keywords: germanium · high-pressure chemistry · magnesium · structure elucidation · superconductors

[1] I. Shin, E. A. Carter, *Acta Mater.* **2014**, *64*, 198 – 207.
[2] V. M. Vidali, *Pure Appl. Chem.* **2001**, *73*, 1163 – 1172.
[3] Y. Noda, H. Kon, Y. Furukawa, N. Otsuka, I. A. Nishida, K. Masumoto, *Mater. Trans. JIM* **1992**, *33*, 845 – 850.
[4] Y. Noda, H. Kon, Y. Furukawa, I. A. Nishida, K. Masumoto, *Mater. Trans. JIM* **1992**, *33*, 851 – 855.
[5] J.-i. Tani, H. Kido, *Physica B + C* **2005**, *364*, 218 – 224.
[6] A. Vantomme, J. E. Mahan, G. Langouche, J. P. Becker, M. Van Bael, K. Temst, C. Van Haesendonck, *Appl. Phys. Lett.* **1997**, *70*, 1086 – 1088.
[7] X. Sauvage, N. Enikeev, R. Valiev, Y. Nasedkina, M. Murashkin, *Acta Mater.* **2014**, *72*, 125 – 136.
[8] T. A. Strobel, O. O. Kurakevych, D. Y. Kim, Y. Le Godec, W. Crichton, J. Guignard, N. Guignot, G. D. Cody, A. R. Oganov, *Inorg. Chem.* **2014**, *53*, 7020 – 7027.
[9] H. Liu, G. Gao, Y. Li, J. Hao, J. S. Tse, *J. Phys. Chem. C* **2015**, *119*, 23168 – 23174.
[10] S. Yu, B. Huang, Q. Zeng, A. R. Oganov, L. Zhang, G. Frapper, *J. Phys. Chem. C* **2017**, *121*, 11037 – 11046.
[11] Q. Zhu, A. R. Oganov, A. O. Lyakhov, *Phys. Chem. Chem. Phys.* **2013**, *15*, 7696 – 7700.
[12] P. Vajeeston, P. Ravindran, B. C. Hauback, H. Fjellvåg, A. Kjekshus, S. Furuseth, M. Hanfland, *Phys. Rev. B* **2006**, *73*, 224102.
[13] D. C. Lonie, J. Hooper, B. Altintas, E. Zurek, *Phys. Rev. B* **2013**, *87*, 054107.
[14] T. D. Huan, *Phys. Rev. Mater.* **2018**, *2*, 023803.
[15] Y. Li, Y. Gao, Y. Han, C. Liu, G. Peng, Q. Wang, F. Ke, Y. Ma, C. Gao, *Appl. Phys. Lett.* **2015**, *107*, 142103.
[16] F. Yu, J.-X. Sun, T.-H. Chen, *Physica B + C* **2011**, *406*, 1789 – 1794.
[17] A. R. Oganov, C. W. Glass, *J. Chem. Phys.* **2006**, *124*, 244704.
[18] A. R. Oganov, A. O. Lyakhov, M. Valle, *Acc. Chem. Res.* **2011**, *44*, 227 – 237.
[19] A. O. Lyakhov, A. R. Oganov, H. T. Stokes, Q. Zhu, *Comput. Phys. Commun.* **2013**, *184*, 1172 – 1182.
[20] Y. Li, H. Wang, Q. Li, Y. Ma, T. Cui, G. Zou, *Inorg. Chem.* **2009**, *48*, 9904 – 9909.
[21] Y. Liu, D. Duan, F. Tian, H. Liu, C. Wang, X. Huang, D. Li, Y. Ma, B. Liu, T. Cui, *Inorg. Chem.* **2015**, *54*, 9924 – 9928.
[22] S. Wei, D. Li, Z. Liu, W. Wang, F. Tian, K. Bao, D. Duan, B. Liu, T. Cui, *J. Phys. Chem. C* **2017**, *121*, 9766 – 9772.
[23] G. Mali, M. U. Patel, M. Mazaj, R. Dominko, *Chemistry* **2016**, *22*, 3355 – 3360.
[24] Y. Yao, J. S. Tse, *Chemistry* **2018**, *24*, 1769 – 1778.
[25] G. Kresse, J. Furthmüller, *Comput. Mater. Sci.* **1996**, *6*, 15 – 50.
[26] J. P. Perdew, K. Burke, M. Ernzerhof, *Phys. Rev. Lett.* **1996**, *77*, 3865.
[27] G. Kresse, D. Joubert, *Phys. Rev. B* **1999**, *59*, 1758.
[28] K. Parlinski, Z. Li, Y. Kawazoe, *Phys. Rev. Lett.* **1997**, *78*, 4063.
[29] A. Togo, F. Oba, I. Tanaka, *Phys. Rev. B* **2008**, *78*, 134106.
[30] A. D. Becke, K. E. Edgecombe, *J. Chem. Phys.* **1990**, *92*, 5397 – 5403.
[31] R. F. Bader, *Acc. Chem. Res.* **1985**, *18*, 9 – 15.
[32] G. Henkelman, A. Arnaldsson, H. Jónsson, *Comput. Mater. Sci.* **2006**, *36*, 354 – 360.
[33] W. Tang, E. Sanville, G. Henkelman, *J. Phys. Condens. Matter* **2009**, *21*, 084204.
[34] P. Giannozzi, S. Baroni, N. Bonini, M. Calandra, R. Car, C. Cavazzoni, D. Ceresoli, G. L. Chiarotti, M. Cococcioni, I. Dabo, A. Dal Corso, S. de Gironcoli, S. Fabris, G. Fratesi, R. Gebauer, U. Gerstmann, C. Gougoussis, A. Kokalj, M. Lazzeri, L. Martin-Samos, N. Marzari, F. Mauri, R. Mazzarello, S. Paolini, A. Pasquarello, L. Paulatto, C. Sbraccia, S. Scandolo, G. Sclauzero, A. P. Seitsonen, A. Smogunov, P. Umari, R. M. Wentzcovitch, *J. Phys. Condens. Matter* **2009**, *21*, 395502.
[35] P. B. Allen, R. C. Dynes, *Phys. Rev. B* **1975**, *12*, 905 – 922.

Manuscript received: August 11, 2018
Accepted manuscript online: October 9, 2018
Version of record online: November 9, 2018